Supplement of Biogeosciences, 23, 4287–4303, 2026
https://doi.org/10.5194/bg-23-4287-2026-supplement

Biogeosciences Open Access EGU

Supplement of

Unlocking the potential of pollarded oaks: a 375-year hydroclimate reconstruction from northcentral Spain

Alba Sanmiguel-Vallelado et al.

Correspondence to: Alba Sanmiguel-Vallelado (alba.sanmiguel@uva.es)

Supplement

Table S1: Sensitivity of the LWI chronology–precipitation relationship to detrending method. Detrending variants were compared against the selected method: a cubic smoothing spline with a 50% frequency-response cutoff at two-thirds of the individual series length, applied without power transformation (non-PT). Fixed-50: cubic smoothing spline with a fixed 50-year frequency cutoff applied regardless of series length. ADC: Age-Dependent Changing Spline, whose rigidity decreases as a function of the number of rings in each series. PT: power transformation applied to raw series prior to detrending to stabilize variance. non-PT: no power transformation applied. Values in the second column are Pearson's correlations between each alternative LWI chronology and the selected LWI chronology, reported for the instrumental period (1902–2022) and the full chronology length (1649–2023), respectively. Remaining columns show Pearson's correlations between each LWI chronology and November–June precipitation from the FIC (1952–2020) and CRU (1952–2020 and 1902–2022) gridded datasets. None of the pairwise differences in climate correlations were statistically significant (Fisher z-test, $p > 0.05$ in all cases).

Detrending method	Selected chronology (1902–2022 / 1649–2023)	FIC (1952–2020)	CRU (1952–2020)	CRU (1902–2020)
Selected: 2/3 spline, non-PT	1.000 / 1.000	0.834	0.832	0.760
Fixed-50, PT	0.958 / 0.927	0.820	0.794	0.746
Fixed-50, non-PT	0.957 / 0.925	0.810	0.790	0.748
ADC, PT	0.928 / 0.834	0.803	0.799	0.733
ADC, non-PT	0.930 / 0.829	0.815	0.777	0.747

Table S2: Running EPS values for the RWI series. Bold font indicates periods with stable EPS values > 0.85. Abbreviations: Start year: first year in the window; End year: last year in the window; N cores: number of cores; N trees: number of trees; N corr: total number of correlations, calculated as the sum of within-tree and between-tree correlations; Rbar: mean correlation among different cores; EPS: expressed population signal; SNR: signal-to-noise ratio.

Start year	End year	N cores	N trees	N corr	Rbar	EPS	SNR
1559	1588	12	12	15	0.197	0.596	1.475
1574	1603	17	17	36	0.207	0.702	2.353
1589	1618	22	22	66	0.212	0.763	3.227
1604	1633	26	26	136	0.131	0.719	2.560
1619	1648	30	30	231	0.210	0.854	5.846
1634	1663	34	34	325	0.161	0.833	5.001
1649	**1678**	**39**	**39**	**435**	**0.175**	**0.864**	**6.348**
1664	**1693**	**43**	**43**	**561**	**0.277**	**0.929**	**13.034**
1679	**1708**	**45**	**45**	**741**	**0.264**	**0.933**	**13.955**
1694	**1723**	**45**	**45**	**946**	**0.209**	**0.921**	**11.594**
1709	**1738**	**46**	**46**	**990**	**0.216**	**0.925**	**12.388**
1724	**1753**	**51**	**51**	**990**	**0.240**	**0.934**	**14.219**
1739	**1768**	**54**	**54**	**1035**	**0.216**	**0.927**	**12.644**
1754	**1783**	**59**	**59**	**1275**	**0.245**	**0.943**	**16.552**
1769	**1798**	**64**	**64**	**1431**	**0.298**	**0.958**	**22.900**
1784	**1813**	**70**	**70**	**1711**	**0.233**	**0.947**	**17.907**
1799	**1828**	**72**	**72**	**2016**	**0.238**	**0.952**	**20.040**
1814	**1843**	**76**	**76**	**2346**	**0.194**	**0.943**	**16.566**
1829	**1858**	**80**	**80**	**2556**	**0.190**	**0.944**	**16.936**

1844	**1873**	**86**	**86**	**2775**	**0.222**	**0.955**	**21.382**
1859	**1888**	**87**	**87**	**3081**	**0.183**	**0.946**	**17.646**
1874	**1903**	**89**	**89**	**3655**	**0.196**	**0.954**	**20.958**
1889	**1918**	**91**	**91**	**3828**	**0.194**	**0.955**	**21.127**
1904	**1933**	**93**	**93**	**3916**	**0.140**	**0.935**	**14.485**
1919	**1948**	**96**	**96**	**4095**	**0.189**	**0.955**	**21.146**
1934	**1963**	**100**	**100**	**4278**	**0.292**	**0.975**	**38.379**
1949	**1978**	**102**	**102**	**4560**	**0.333**	**0.980**	**47.884**
1964	**1993**	**102**	**102**	**5050**	**0.380**	**0.984**	**61.775**
1979	**2008**	**102**	**102**	**5151**	**0.426**	**0.987**	**75.668**
1994	**2023**	**102**	**102**	**45**	**0.372**	**0.856**	**5.935**

Table S3: Running EPS values for the EWI series. Bold font: periods showing a stabilized EPS > 0.85. Abbreviations: Start year: the first year in the window; End year: the last year in the window; N cores: the number of cores; N trees: the number of trees; N corr: total number of correlations as number of within-tree + between-tree correlations computed; Rbar: mean of all the correlations between different cores; EPS: Expressed Population Signal; SNR: Signal-to-Noise Ratio.

Start year	End year	N cores	N trees	N corr	Rbar	EPS	SNR
1559	1588	12	12	15	0.015	0.085	0.093
1574	1603	17	17	36	0.073	0.415	0.709
1589	1618	22	22	66	0.116	0.611	1.572
1604	1633	26	26	136	0.030	0.347	0.532
1619	1648	30	30	231	0.071	0.626	1.672
1634	1663	34	34	325	0.049	0.572	1.338
1649	1678	39	39	435	0.076	0.712	2.473
1664	1693	43	43	561	0.145	0.852	5.761
1679	1708	45	45	741	0.150	0.873	6.895
1694	1723	45	45	946	0.099	0.829	4.860
1709	1738	46	46	990	0.073	0.779	3.534
1724	1753	51	51	990	0.076	0.786	3.676
1739	1768	54	54	1035	0.086	0.812	4.306
1754	1783	59	59	1275	0.079	0.813	4.358
1769	**1798**	**64**	**64**	**1431**	**0.152**	**0.906**	**9.664**
1784	**1813**	**70**	**70**	**1711**	**0.107**	**0.876**	**7.037**
1799	**1828**	**72**	**72**	**2016**	**0.097**	**0.873**	**6.849**
1814	**1843**	**76**	**76**	**2346**	**0.089**	**0.871**	**6.760**
1829	**1858**	**80**	**80**	**2556**	**0.093**	**0.881**	**7.422**
1844	**1873**	**86**	**86**	**2775**	**0.102**	**0.895**	**8.486**
1859	**1888**	**87**	**87**	**3081**	**0.100**	**0.898**	**8.819**
1874	**1903**	**89**	**89**	**3655**	**0.110**	**0.914**	**10.647**
1889	**1918**	**91**	**91**	**3828**	**0.105**	**0.911**	**10.277**
1904	**1933**	**93**	**93**	**3916**	**0.049**	**0.822**	**4.609**
1919	**1948**	**96**	**96**	**4095**	**0.066**	**0.865**	**6.399**
1934	**1963**	**100**	**100**	**4278**	**0.107**	**0.917**	**11.088**
1949	**1978**	**102**	**102**	**4560**	**0.140**	**0.940**	**15.641**

1964	**1993**	**102**	**102**	**5050**	**0.139**	**0.942**	**16.267**
1979	**2008**	**102**	**102**	**5151**	**0.183**	**0.958**	**22.843**
1994	**2023**	**102**	**102**	**45**	**0.179**	**0.686**	**2.183**

Table S4: Running EPS values for the LWI series. Bold font: periods showing a stabilized EPS > 0.85. Abbreviations: Start year: the first year in the window; End year: the last year in the window; N cores: the number of cores; N trees: the number of trees; N corr: total number of correlations as number of within-tree + between-tree correlations computed; Rbar: mean of all the correlations between different cores; EPS: Expressed Population Signal; SNR: Signal-to-Noise Ratio.

Start year	End year	N cores	N trees	N corr	Rbar	EPS	SNR
1559	1588	12	12	15	0.182	0.571	1.333
1574	1603	17	17	36	0.202	0.695	2.279
1589	1618	21	21	66	0.182	0.728	2.672
1604	1633	25	25	136	0.158	0.761	3.193
1619	1648	29	29	210	0.198	0.838	5.184
1634	1663	33	33	300	0.177	0.843	5.364
1649	**1678**	**38**	**38**	**406**	**0.213**	**0.887**	**7.843**
1664	**1693**	**42**	**42**	**528**	**0.295**	**0.933**	**13.838**
1679	**1708**	**44**	**44**	**703**	**0.249**	**0.926**	**12.598**
1694	**1723**	**45**	**45**	**903**	**0.196**	**0.913**	**10.506**
1709	**1738**	**46**	**46**	**946**	**0.221**	**0.926**	**12.491**
1724	**1753**	**51**	**51**	**990**	**0.260**	**0.941**	**15.847**
1739	**1768**	**54**	**54**	**1035**	**0.228**	**0.931**	**13.598**
1754	**1783**	**59**	**59**	**1275**	**0.237**	**0.941**	**15.821**
1769	**1798**	**64**	**64**	**1431**	**0.237**	**0.944**	**16.739**
1784	**1813**	**70**	**70**	**1711**	**0.226**	**0.945**	**17.198**
1799	**1828**	**72**	**72**	**2016**	**0.234**	**0.951**	**19.503**
1814	**1843**	**76**	**76**	**2346**	**0.178**	**0.937**	**14.967**
1829	**1858**	**80**	**80**	**2556**	**0.168**	**0.936**	**14.541**
1844	**1873**	**86**	**86**	**2775**	**0.200**	**0.949**	**18.726**
1859	**1888**	**87**	**87**	**3081**	**0.150**	**0.933**	**13.956**
1874	**1903**	**89**	**89**	**3655**	**0.159**	**0.942**	**16.278**
1889	**1918**	**91**	**91**	**3828**	**0.167**	**0.947**	**17.702**
1904	**1933**	**93**	**93**	**3916**	**0.143**	**0.937**	**14.907**
1919	**1948**	**96**	**96**	**4095**	**0.196**	**0.957**	**22.148**
1934	**1963**	**100**	**100**	**4278**	**0.290**	**0.974**	**37.942**
1949	**1978**	**102**	**102**	**4560**	**0.306**	**0.977**	**42.231**
1964	**1993**	**102**	**102**	**5050**	**0.341**	**0.981**	**52.229**
1979	**2008**	**102**	**102**	**5151**	**0.387**	**0.985**	**64.357**
1994	**2023**	**102**	**102**	**45**	**0.452**	**0.892**	**8.236**

Table S5: Effects of pollarding on precipitation signals: results from the RWI linear mixed-effects model. Fixed effects: November–June precipitation (CRU data, 1902–2022) and time since pollarding. Random effects: the individual sampled trees (N = 93); σ^2 = 0.06. Observations = 6708. Marginal R^2 = 0.245; Conditional R^2 = 0.249. CI: confidence interval.

Predictors	Estimates	CI	p-value
(Intercept)	0.79059	0.66120 – 0.91997	<0.001
pp rwi	0.00088	0.00062 – 0.00114	<0.001
time [1]	-0.09783	-0.28727 – 0.09161	0.311
time [2]	-0.12816	-0.31943 – 0.06310	0.189
time [3]	-0.24495	-0.43954 – -0.05037	0.014
time [4]	-0.36922	-0.56703 – -0.17141	<0.001
time [5]	-0.35584	-0.55709 – -0.15460	0.001
time [6]	-0.14759	-0.33529 – 0.04010	0.123
time [7]	-0.30347	-0.51550 – -0.09143	0.005
time [8]	-0.4105	-0.61363 – -0.20737	<0.001
time [9]	-0.27058	-0.46686 – -0.07430	0.007
time [10]	-0.28611	-0.41948 – -0.15273	<0.001
pp rwi × time [1]	-0.00034	-0.00075 – 0.00008	0.112
pp rwi × time [2]	-0.00061	-0.00103 – -0.00018	0.005
pp rwi × time [3]	-0.00028	-0.00071 – 0.00014	0.194
pp rwi × time [4]	0.00003	-0.00038 – 0.00045	0.881
pp rwi × time [5]	0.00014	-0.00028 – 0.00056	0.511
pp rwi × time [6]	-0.00027	-0.00068 – 0.00013	0.187
pp rwi × time [7]	0.0002	-0.00025 – 0.00066	0.383
pp rwi × time [8]	0.00053	0.00009 – 0.00097	0.018
pp rwi × time [9]	0.00023	-0.00021 – 0.00066	0.303
pp rwi × time [10]	0.00032	0.00005 – 0.00059	0.021

Table S6: Influence of pollarding on precipitation signals: results from the EWI linear mixed-effects model. Fixed effects: November–February precipitation (CRU data, 1902–2022) and time since pollarding. Random effects: the individual sampled trees (N = 93); σ^2 = 0.05. Observations = 6726. Marginal R^2 = 0.061; Conditional R^2 = 0.062. CI: confidence interval.

Predictors	Estimates	CI	p-value
(Intercept)	0.83659	0.75025 – 0.92294	<0.001
pp ewi	0.00074	0.00039 – 0.00109	<0.001
time [1]	0.03264	-0.09473 – 0.16001	0.615
time [2]	0.03777	-0.08248 – 0.15802	0.538
time [3]	-0.01363	-0.14047 – 0.11321	0.833
time [4]	-0.12094	-0.25491 – 0.01304	0.077
time [5]	-0.08716	-0.22017 – 0.04585	0.199
time [6]	0.05555	-0.07039 – 0.18148	0.387
time [7]	0.03131	-0.10284 – 0.16546	0.647
time [8]	0.00879	-0.12193 – 0.13951	0.895
time [9]	0.03283	-0.09596 – 0.16162	0.617
time [10]	0.04401	-0.04491 – 0.13293	0.332
pp ewi × time [1]	0.00007	-0.00048 – 0.00063	0.791

pp ewi × time [2]	-0.00035	-0.00088 – 0.00017	0.187
pp ewi × time [3]	-0.00028	-0.00083 – 0.00027	0.318
pp ewi × time [4]	0.000003	-0.00055 – 0.00055	0.991
pp ewi × time [5]	0.00006	-0.00048 – 0.00061	0.821
pp ewi × time [6]	-0.00042	-0.00095 – 0.00011	0.123
pp ewi × time [7]	-0.00023	-0.00080 – 0.00034	0.422
pp ewi × time [8]	-0.00008	-0.00064 – 0.00047	0.775
pp ewi × time [9]	-0.00009	-0.00066 – 0.00048	0.76
pp ewi × time [10]	-0.0001	-0.00047 – 0.00026	0.569

Table S7: Influence of pollarding on precipitation signals: results from the LWI linear mixed-effects model. Fixed effects: November–June precipitation (CRU data, 1902–2022) and time since pollarding. Random effects: the individual sampled trees (N = 93); $\sigma^2 = 0.22$. Observations = 6726. Marginal $R^2 = 0.284$; Conditional $R^2 = 0.286$. CI: confidence interval.

Predictors	Estimates	CI	p-value
(Intercept)	0.83852	0.59589 – 1.08114	<0.001
pp lwi	0.00158	0.00109 – 0.00207	<0.001
time [1]	-0.40885	-0.76754 – -0.05015	0.025
time [2]	-0.57884	-0.94100 – -0.21669	0.002
time [3]	-0.54786	-0.91571 – -0.18001	0.004
time [4]	-0.78633	-1.15985 – -0.41281	<0.001
time [5]	-0.77853	-1.15880 – -0.39826	<0.001
time [6]	-0.68271	-1.03804 – -0.32738	<0.001
time [7]	-0.87925	-1.28130 – -0.47720	<0.001
time [8]	-1.07826	-1.46238 – -0.69413	<0.001
time [9]	-0.79045	-1.16223 – -0.41868	<0.001
time [10]	-0.84514	-1.09551 – -0.59478	<0.001
pp lwi × time [1]	-0.00091	-0.00170 – -0.00013	0.022
pp lwi × time [2]	-0.00112	-0.00193 – -0.00032	0.006
pp lwi × time [3]	-0.0009	-0.00171 – -0.00009	0.029
pp lwi × time [4]	-0.00007	-0.00085 – 0.00072	0.864
pp lwi × time [5]	0.00011	-0.00068 – 0.00091	0.785
pp lwi × time [6]	-0.00004	-0.00081 – 0.00072	0.91
pp lwi × time [7]	0.00062	-0.00025 – 0.00148	0.16
pp lwi × time [8]	0.00129	0.00046 – 0.00213	0.002
pp lwi × time [9]	0.00056	-0.00026 – 0.00138	0.178
pp lwi × time [10]	0.00082	0.00031 – 0.00133	0.002

Table S8: Calibration–validation schemes tested for the November–June precipitation reconstruction model.

Scheme	CALIBRATION			VALIDATION					
	Calibration dataset	Calibration period	Adjusted R^2	Validation dataset	Validation period	r	RE	CE	RMSE (mm)
Late FIC calibration – Early CRU validation	FIC	1962–2020	0.70	CRU	1902–1961	0.71	0.44	0.45	76.21
Late CRU calibration – Early CRU validation	CRU	1962–2022	0.69	CRU	1902–1961	0.71	0.44	0.45	76.21
Early CRU calibration – Late CRU validation	CRU	1902–1961	0.48	CRU	1962–2022	0.83	0.67	0.67	53.75
Early FIC calibration – Late FIC validation	FIC	1952–1986	0.67	FIC	1987–2020	0.84	0.68	0.68	77.60

Note: adjusted R^2 = adjusted coefficient of determination; r = Pearson's correlation coefficient; RE = reduction of error; CE = coefficient of efficiency; RMSE = root-mean-square error.

Table S9: Extreme years identified in the raw and bias-corrected November–June precipitation reconstructions. The table includes all years flagged as extreme by at least one of the three threshold criteria (±1.5 SD, 5th/95th percentiles, SPI categories), indicating which criterion or criteria detected each year, agreement between raw and bias-corrected reconstructions, reconstructed precipitation in both series, and SPI values. Dry years are ordered from lower to higher precipitation and wet years from higher to lower precipitation.

Extreme type	Year	Detected in both reconstructions?	Method(s)	Bias-corrected precipitation (mm)	Raw precipitation (mm)	SPI
Dry	1683	Yes	mean-1.5 SD; P5; SPI	257	273	-1.92
	1734	Yes	mean-1.5 SD; P5; SPI	258	275	-2.09
	2012	Yes	mean-1.5 SD; P5; SPI	265	287	-1.70
	1995	Yes	mean-1.5 SD; P5; SPI	276	303	-1.66
	2005	Yes	mean-1.5 SD; P5; SPI	276	304	-1.88
	1737	Yes	mean-1.5 SD; P5; SPI	288	322	-1.67
	1775	Yes	mean-1.5 SD; P5; SPI	288	322	-1.93
	1999	Yes	mean-1.5 SD; P5; SPI	290	325	-1.83
	1868	Yes	mean-1.5 SD; P5	290	325	-1.42
	1981	Yes	P5; SPI	294	331	-1.58
	1698	Yes	P5; SPI	295	334	-1.54

	1949	Yes	P5; SPI	296	335	-1.96
	1738	Yes	P5	298	337	-1.41
	1898	Yes	P5; SPI	298	338	-1.56
	1767	Yes	P5	303	346	-1.30
	1718	Yes	P5	304	348	-1.47
	1844	Yes	P5	305	349	-1.26
	1665	Yes	P5	312	360	-1.32
	1833	Yes	P5	315	364	-1.28
	1803	No (raw only)	mean-1.5 SD	316	366	-1.14
	1687	No (raw only)	SPI	318	369	-1.44
	1699	No (raw only)	SPI	319	370	-1.43
	1744	No (raw only)	SPI	320	372	-1.46
	1828	No (raw only)	SPI	324	377	-1.42
	1811	No (raw only)	SPI	327	383	-1.38
	1896	No (raw only)	SPI	329	385	-1.40
	1757	Yes	SPI	329	385	-1.50
	1824	No (raw only)	SPI	329	386	-1.39
	1684	Yes	mean+1.5 SD; P95; SPI	838	857	3.01
	1784	Yes	mean+1.5 SD; P95; SPI	771	804	2.19
	1988	Yes	mean+1.5 SD; P95; SPI	754	791	2.10
	1708	Yes	mean+1.5 SD; P95; SPI	750	788	2.41
	1966	Yes	mean+1.5 SD; P95; SPI	748	786	2.58
	1930	Yes	mean+1.5 SD; P95; SPI	734	775	2.48
Wet	1977	Yes	mean+1.5 SD; P95; SPI	711	757	2.84
	1692	Yes	mean+1.5 SD; P95; SPI	711	757	2.16
	1800	Yes	mean+1.5 SD; P95; SPI	676	730	1.90
	1795	Yes	mean+1.5 SD; P95; SPI	674	728	2.19
	1736	Yes	mean+1.5 SD; P95	664	721	1.56
	1799	Yes	mean+1.5 SD; P95; SPI	657	715	2.00
	1848	Yes	mean+1.5 SD; P95	629	693	1.53
	2021	Yes	mean+1.5 SD; P95; SPI	628	692	1.68

	1814	Yes	mean+1.5 SD; P95; SPI	626	690	2.15
	1735	Yes	mean+1.5 SD; P95; SPI	624	689	1.78
	1763	Yes	mean+1.5 SD; P95	605	674	1.56
	1731	Yes	mean+1.5 SD; P95	603	673	1.66
	1670	Yes	mean+1.5 SD; P95; SPI	601	671	1.92
	1860	No (bias-corrected only)	mean+1.5 SD	600	670	1.29
	1721	No (bias-corrected only)	mean+1.5 SD	596	667	1.40
	1762	No (bias-corrected only)	mean+1.5 SD	596	667	1.47
	1758	Yes	SPI	594	666	1.74
	1877	No (bias-corrected only)	mean+1.5 SD	589	662	1.34
	1985	No (bias-corrected only)	mean+1.5 SD	588	660	1.32
	1915	No (bias-corrected only)	mean+1.5 SD	586	659	1.44
	1746	No (bias-corrected only)	SPI	583	657	1.64
	1782	No (bias-corrected only)	SPI	569	646	1.51
	2013	No (bias-corrected only)	SPI	568	646	1.59
	1969	No (bias-corrected only)	SPI	539	622	1.68
	1861	No (bias-corrected only)	SPI	535	619	1.64
	1657	No (bias-corrected only)	SPI	528	613	1.56

Table S10: Wet and dry periods identified in the bias-corrected November–June precipitation reconstruction (1649–2023) for northcentral Spain. Bold font indicates the pre-instrumental period.

Period	Start year	End year	Mean precipitation (mm)	Duration (years)
	1702	**1712**	456	**11**
	1719	**1739**	465	**21**
	1756	**1769**	474	**14**
Wet	**1793**	**1804**	461	**12**
	1806	**1818**	455	**13**
	1855	**1864**	452	**10**
	1924	1938	460	15

	1953	1970	478	18
	1971	1981	450	11
Dry	**1652**	**1669**	400	**18**
	1739	**1756**	419	**18**
	1769	**1778**	423	**10**
	1818	**1842**	412	**25**
	1864	**1879**	421	**16**
	1881	**1897**	434	**17**
	1938	1949	412	12
	2005	2015	424	11

Table S11: Correspondence between extreme dry years in the bias-corrected November–June precipitation reconstruction (1649–2023) for northcentral Spain and historical documentary records. The table includes all years identified as dry extremes by at least one of the three threshold criteria (±1.5 SD, 5th/95th percentiles, SPI categories). Bold font indicates the pre-instrumental period.

Extreme dry year	Documentary record
1665	**Although no rogation record was found for 1665 itself, the marked precipitation decline in the reconstruction and the occurrence of documented drought-related rogations in nearby Valladolid and Zamora in 1664 and 1666 suggest that 1665 formed part of a short regional drought episode (Bellido Blanco, 2017; Domínguez-Castro et al., 2010).**
1683	***Pro pluvia* rogation in Valladolid performed in April (Bellido Blanco, 2017); Historical drought affecting most of peninsular Spain (Centro de Estudios Hidrográficos, 2013).**
1698	***Pro pluvia* rogation in Valladolid performed in May (Bellido Blanco, 2017); *Pro pluvia* rogation in Zamora performed in spring (Domínguez-Castro et al., 2010); Historical drought affecting most of peninsular Spain (Centro de Estudios Hidrográficos, 2013).**
1718	***Pro pluvia* rogation in Tordesillas performed in May (Bellido Blanco, 2017); Historical drought affecting Castilla, Aragón-Monegros, Levante, Urgel, the Segura basin, and the southern half of the Iberian Peninsula (Centro de Estudios Hidrográficos, 2013).**
1734	***Pro pluvia* rogation in Valladolid performed in May (Bellido Blanco, 2017); Historical drought affecting Castile, Aragon, and Andalusia (Centro de Estudios Hidrográficos, 2013).**
1737	***Pro pluvia* rogation in Valladolid performed in April (Bellido Blanco, 2017); *Pro pluvia* rogation in Zamora performed in winter (Domínguez-Castro et al., 2010); Historical drought affecting most of peninsular Spain (Centro de Estudios Hidrográficos, 2013).**
1738	**Two *pro pluvia* rogations in Valladolid performed in May (Bellido Blanco, 2017); One *pro pluvia* rogation in Zamora performed in winter and another one in spring (Domínguez-Castro et al., 2010); Historical drought affecting most of peninsular Spain (Centro de Estudios Hidrográficos, 2013).**
1757	***Pro pluvia* rogation in Zamora performed in spring (Domínguez-Castro et al., 2012); Historical drought affecting the Meseta and Levante (Centro de Estudios Hidrográficos, 2013).**
1767	**Three *pro pluvia* rogations in Valladolid and one in Cuéllar all performed in May (Bellido Blanco, 2017); *Pro pluvia* rogation in Zamora performed in spring (Domínguez-Castro et al., 2012); Historical drought affecting Castilla and Aragón (Centro de Estudios Hidrográficos, 2013).**

1775	**Three *pro pluvia* rogations in Valladolid performed in May (Bellido Blanco, 2017); *Pro pluvia* rogation in Zamora performed in spring (Domínguez-Castro et al., 2012); Historical drought affecting Castile (Centro de Estudios Hidrográficos, 2013).**
1833	***Pro pluvia* rogation in Zamora performed in spring (Domínguez-Castro et al., 2012).**
1844	***Pro pluvia* rogation in Valladolid performed in April (Bellido Blanco, 2017).**
1868	**Two *pro pluvia* rogations in Valladolid performed in April (Bellido Blanco, 2017); Historical drought affecting most of peninsular Spain (Centro de Estudios Hidrográficos, 2013).**
1898	**Historical drought affecting most of peninsular Spain (Centro de Estudios Hidrográficos, 2013).**
1949	Spanish Drought Catalogue (Trullenque-Blanco et al., 2024).
1981	Spanish Drought Catalogue (Trullenque-Blanco et al., 2024).
1995	Spanish Drought Catalogue (Trullenque-Blanco et al., 2024).
1999	Spanish Drought Catalogue (Trullenque-Blanco et al., 2024).
2005	Spanish Drought Catalogue (Trullenque-Blanco et al., 2024).
2012	Spanish Drought Catalogue (Trullenque-Blanco et al., 2024).

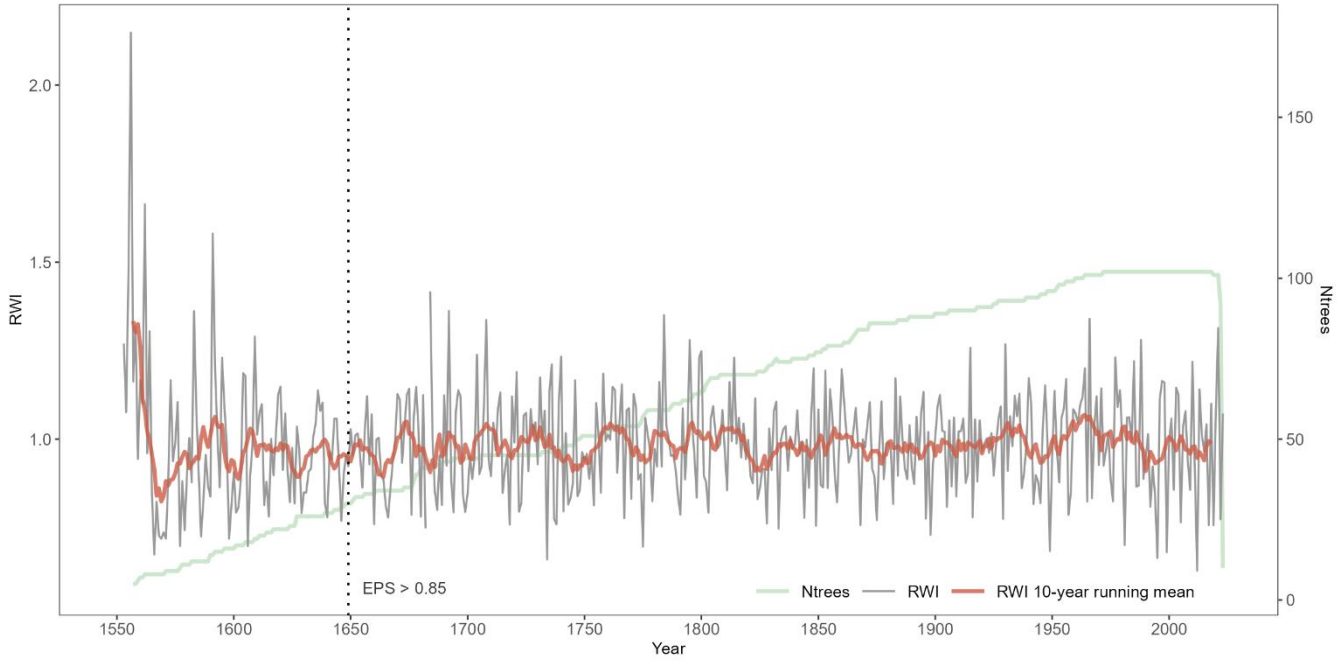

Figure S1: RWI chronology and sample depth.

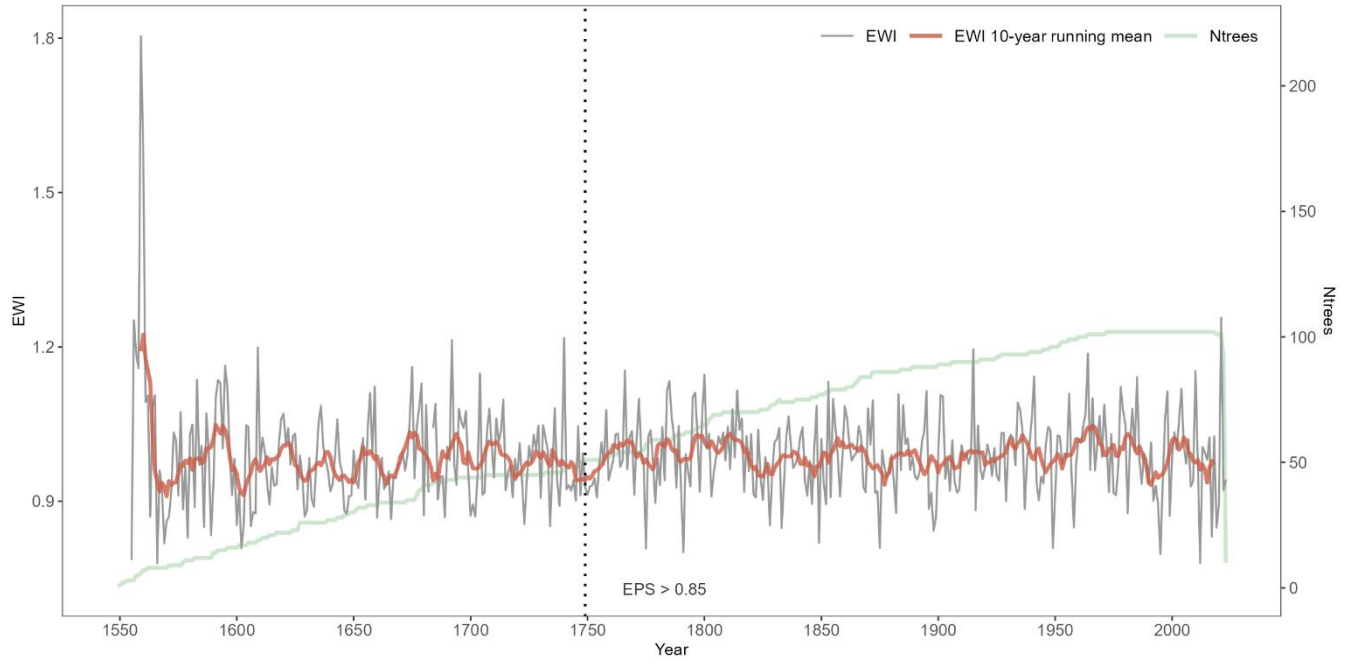

Figure S2: EWI chronology and sample depth.

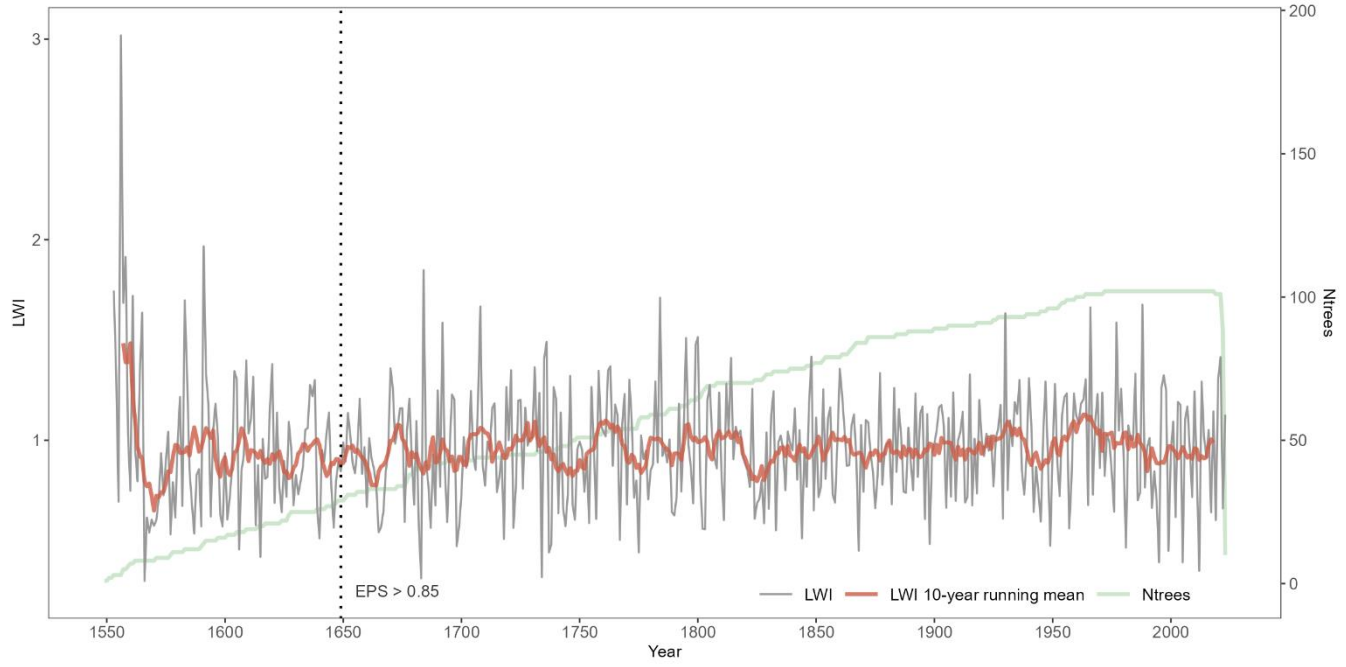

Figure S3: LWI chronology and sample depth.

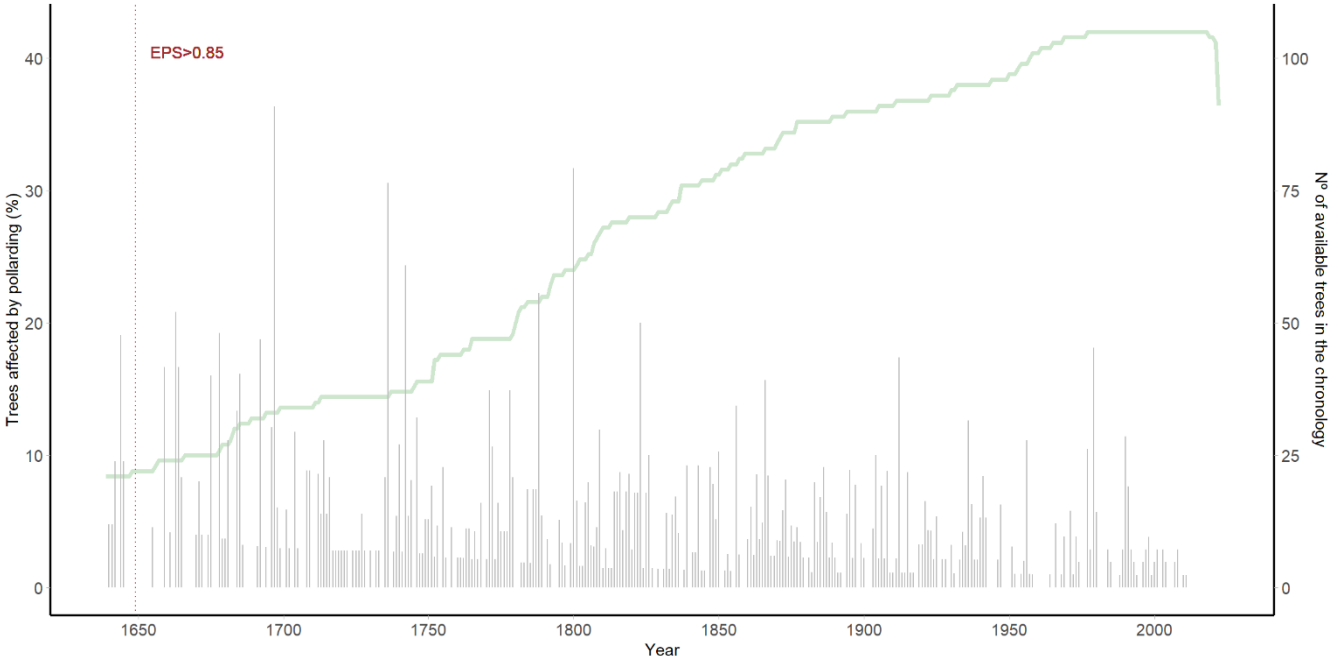

Figure S4: Percentage of trees affected by pollarding events each year (grey segments) relative to the number of trees available in the chronology at that time (green line), based on Sanmiguel-Vallelado et al. (2024).

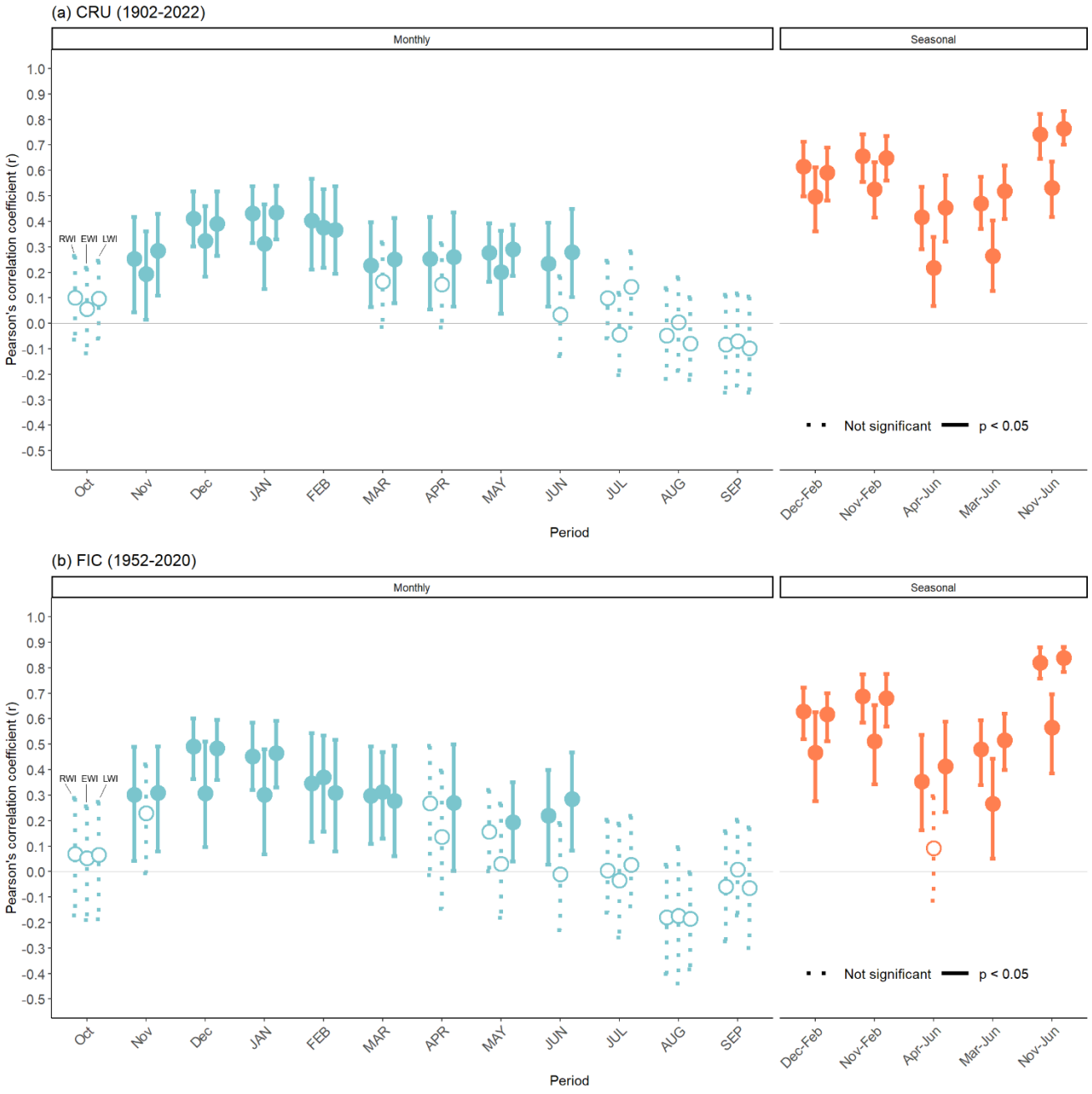

Figure S5: Monthly and seasonal Pearson's correlation coefficients between site chronologies (RWI, EWI, and LWI) and (a) CRU precipitation (1902–2022) or (b) FIC precipitation (1952–2020). Months in lowercase refer to the previous year, whereas months in uppercase refer to the current year.

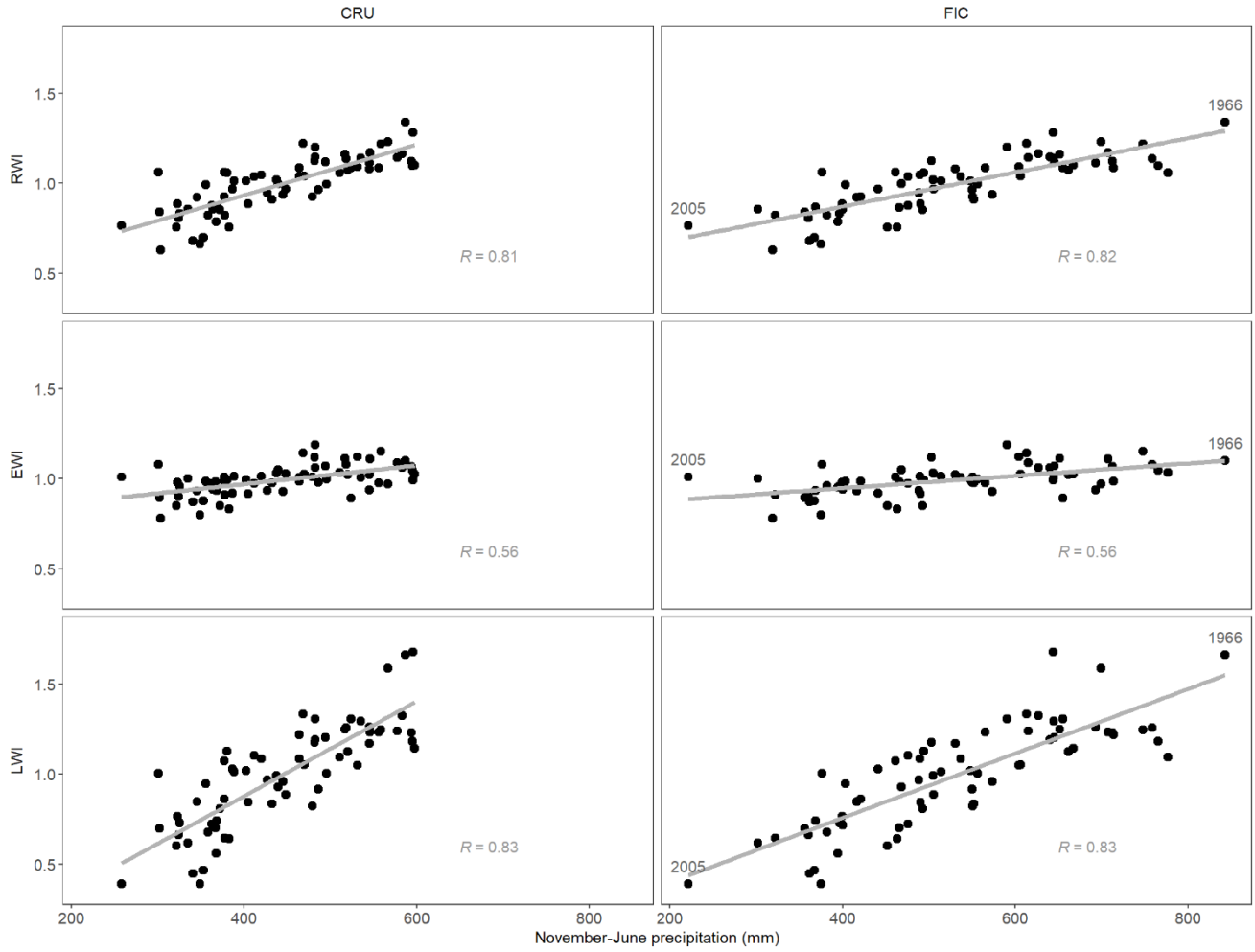

85 **Figure S6: Scatterplots showing the relationship between November–June precipitation and the site chronologies for RWI (top), EWI (middle), and LWI (bottom). Left panels use CRU precipitation data; right panels use FIC precipitation data. All correlations were computed over the common period covered by both datasets (1952–2020).**

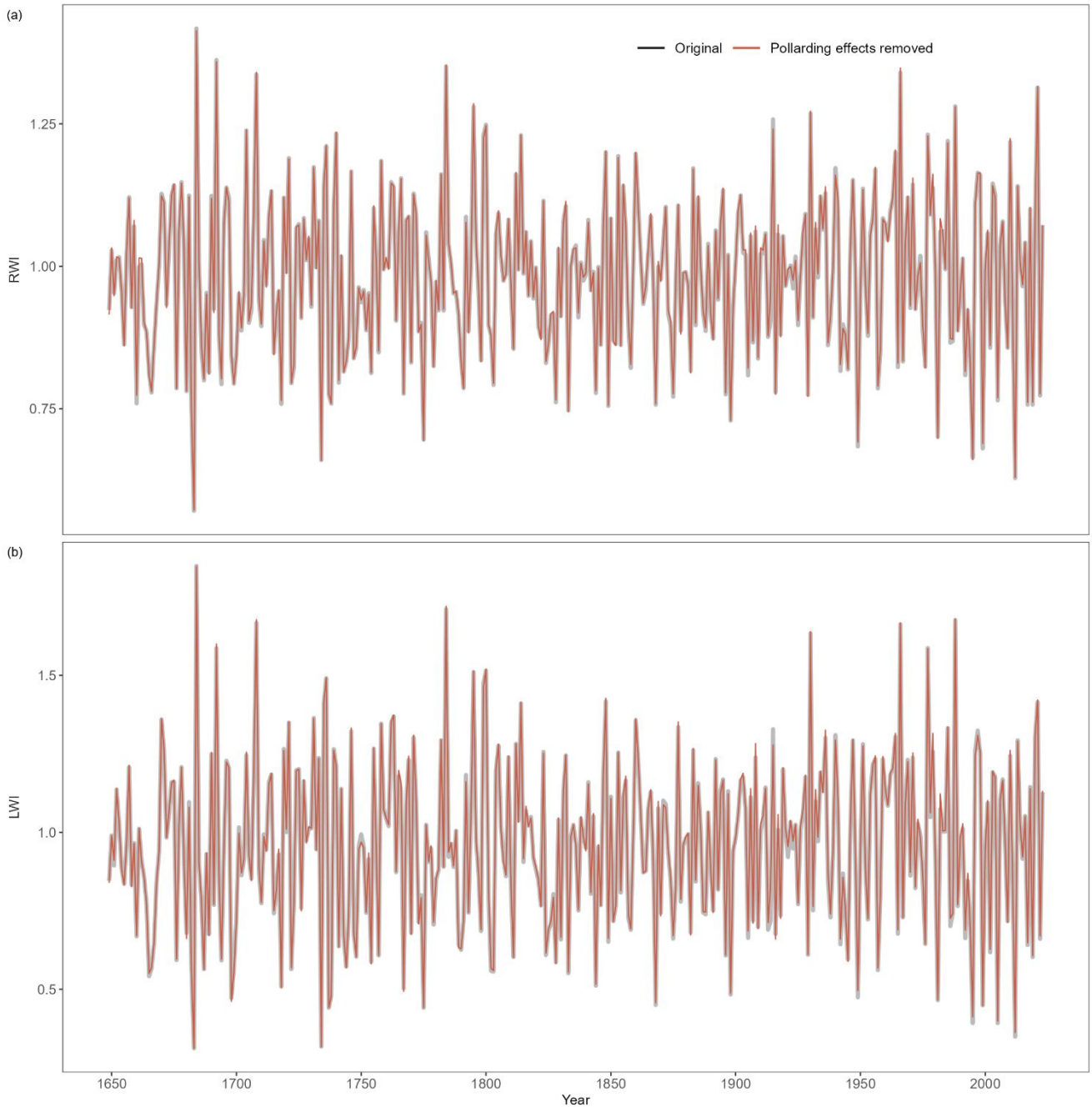

Figure S7: Comparison of RWI (a) and LWI (b) site chronologies before and after removing the effects of pollarding.

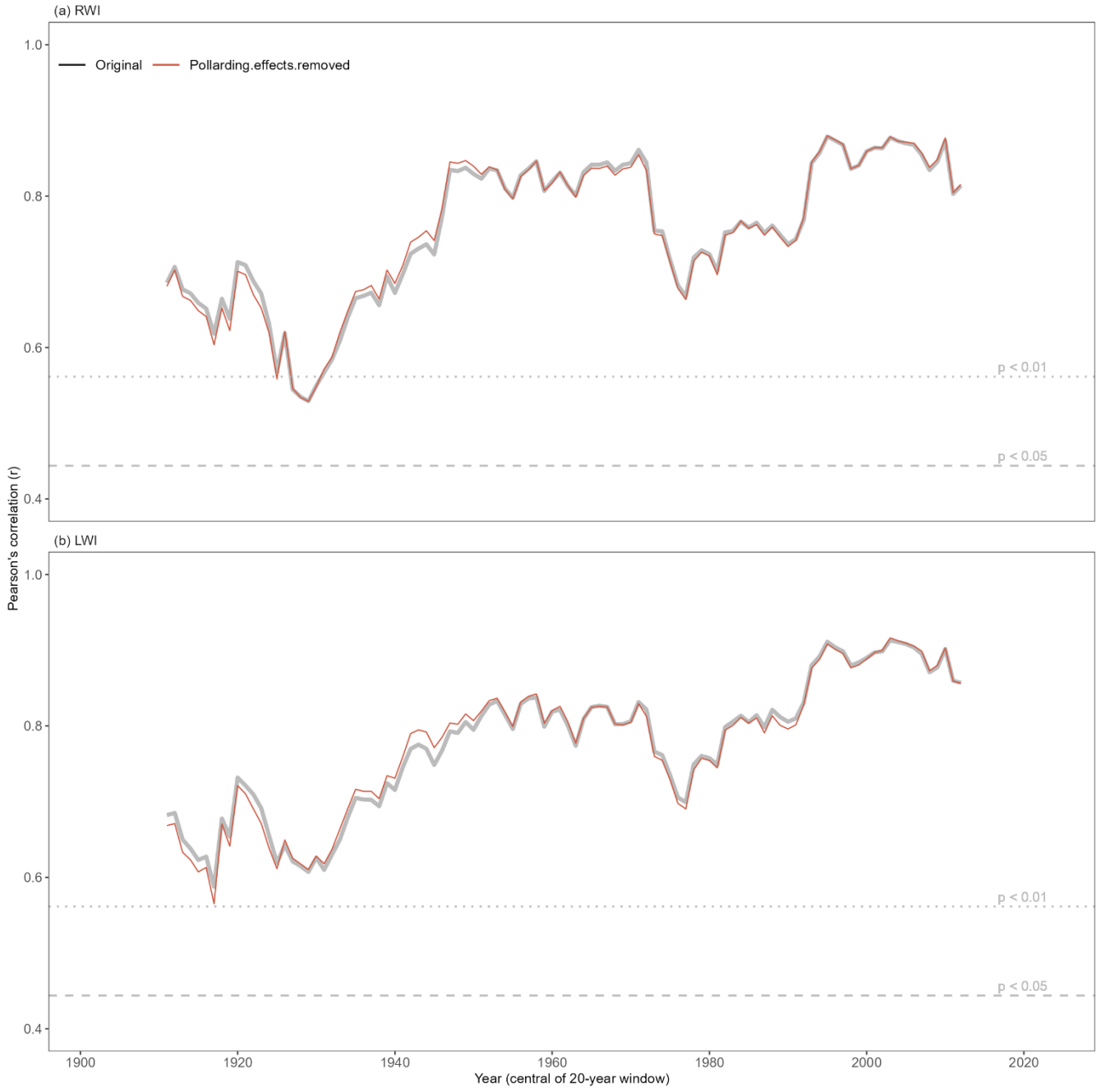

Figure S8: Stability of the dendroclimatic relationship between November–June precipitation and site chronologies before and after removing the effects of pollarding. Precipitation data source: CRU (1902–2022). Panels show the RWI (a) and LWI (b) chronologies. Pearson's r was calculated using a 20-year moving window.

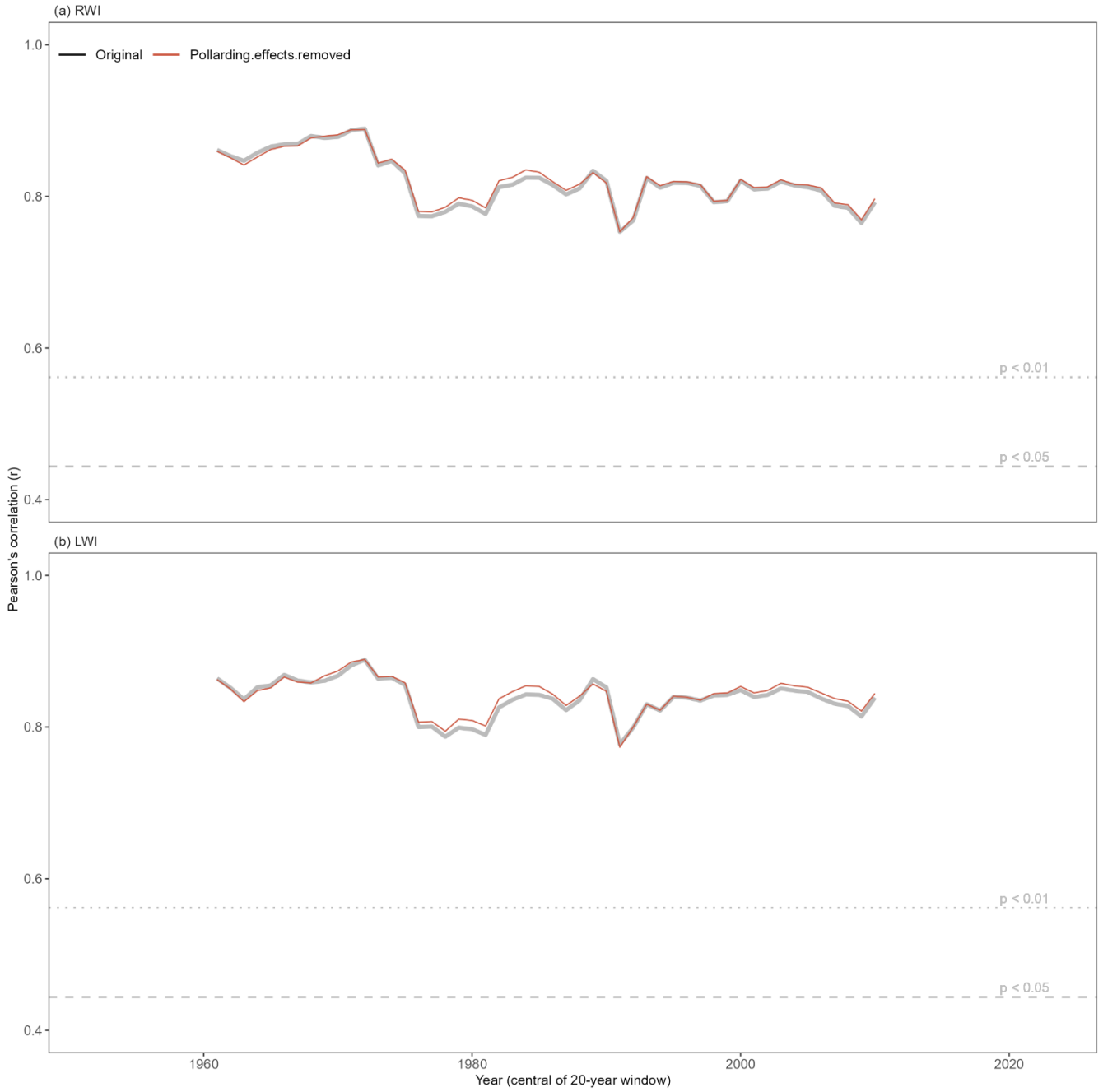

Figure S9: Stability of the dendroclimatic relationship between November–June precipitation and site chronologies before and after removing the effects of pollarding. Precipitation data source: FIC (1952–2020). Panels show the RWI (a) and LWI (b) chronologies. Pearson's r was calculated using a 20-year moving window.

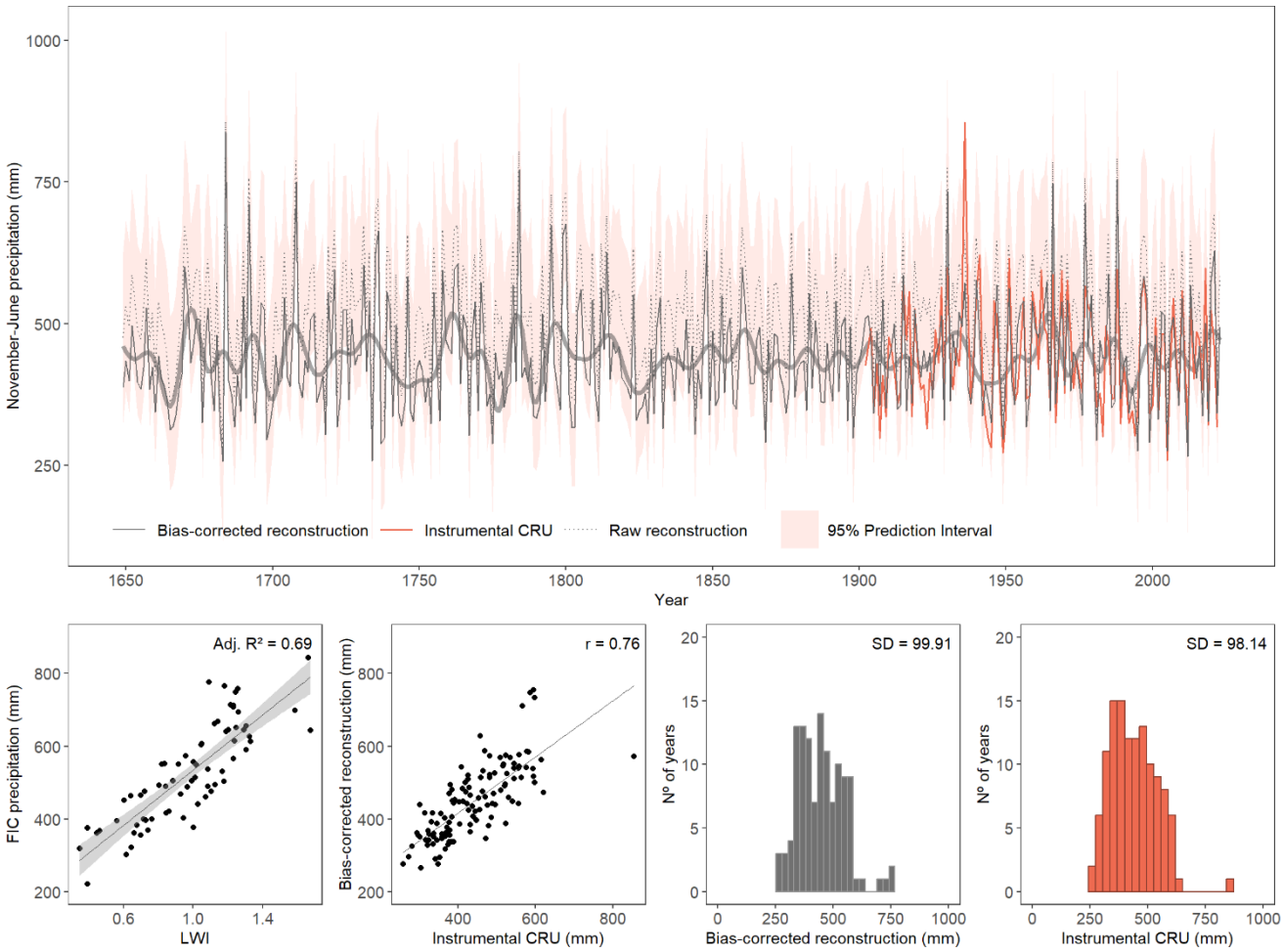

105

Figure S10: (a) Reconstructed November–June precipitation from 1649 to 2023 derived from pollarded oak LWI data in northcentral Spain. The grey curve shows interannual variability; the shaded area represents the 95% prediction interval of the final calibration model using the full FIC precipitation series (1952–2020). A band-pass filter was applied to isolate low-frequency variability by retaining periodicities between 10 and 100 years (thick line). The reconstruction is compared with the full CRU
110 **precipitation series (1902–2022; orange line) to assess its consistency (see Fig. 5 for the split calibration–validation approach). (b) Scatterplot with linear regression between the LWI chronology and full FIC precipitation (1952–2020; final calibration). (c) Scatterplot showing the relationship between full CRU and the bias-corrected reconstruction (1902–2022). (d–e) Frequency distributions of bias-corrected reconstruction and full CRU precipitation, respectively (1902–2022).**

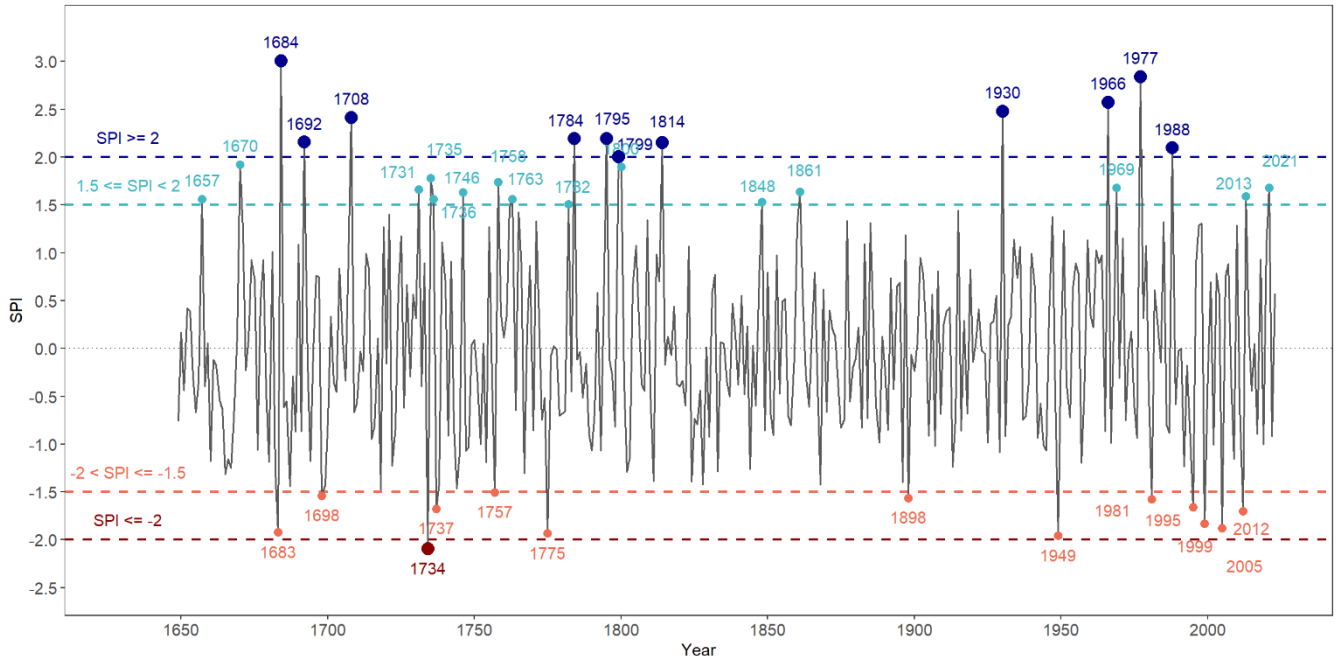

Figure S11: Extreme wet and dry years identified in the bias-corrected November–June precipitation reconstruction (1649–2023) using Standardized Precipitation Index (SPI) categories. See Figure 6 for extremes identified under the ±1.5 SD and 5th/95th percentile criteria.

References

Bellido Blanco, A.: Pidiendo ayuda a los cielos: rogativas en la provincia de Valladolid, Ediciones Universidad de Valladolid, 2017.

Centro de Estudios Hidrográficos: Catálogo y Publicación sobre Sequías Históricas, Ministerio de Agricultura, Alimentación y Medio Ambiente. Secretaría de Estado de Medio Ambiente. Dirección General del Agua., Madrid, 2013.

Domínguez-Castro, F., García-Herrera, R., Ribera, P., and Barriendos, M.: A shift in the spatial pattern of Iberian droughts during the 17th century, Clim. Past, 6, 553–563, https://doi.org/10.5194/cp-6-553-2010, 2010.

Domínguez-Castro, F., Ribera, P., García-Herrera, R., Vaquero, J. M., Barriendos, M., Cuadrat, J. M., and Moreno, J. M.: Assessing extreme droughts in Spain during 1750–1850 from rogation ceremonies, Clim. Past, 8, 705–722, https://doi.org/10.5194/cp-8-705-2012, 2012.

Trullenque-Blanco, V., Beguería, S., Vicente-Serrano, S. M., Peña-Angulo, D., and González-Hidalgo, C.: Catalogue of drought events in peninsular Spanish along 1916–2020 period, Sci Data, 11, 703, https://doi.org/10.1038/s41597-024-03484-w, 2024.